

Kinetics of the reactive absorption of carbon dioxide in high CO₂-loaded, concentrated aqueous monoethanolamine solutions

Ahmed Aboudheir^a, Paitoon Tontiwachwuthikul^{a,*}, Amit Chakma^b, Raphael Idem^a

^aFaculty of Engineering, University of Regina, Regina, SK, Canada S4S 0A2

^bUniversity of Waterloo, Waterloo, ON, Canada N2L 3G1

Received 10 January 2003; accepted 12 August 2003

Abstract

The kinetics of the reaction between carbon dioxide and high CO₂-loaded, concentrated aqueous solutions of monoethanolamine (MEA) were investigated over the temperature range from 293 to 333 K, MEA concentration range from 3 to 9M, and CO₂ loading from ~ 0.1 to 0.49 mol/mol. The experimental kinetic data were obtained in a laminar jet absorber at various contact-times between gas and liquid. The obtained experimental data were interpreted with the aid of a numerically solved absorption-rate/kinetic model. The results showed that only the termolecular mechanism of Crooks and Donnellan could be used to explain all observed kinetic phenomena. These results allowed us to develop a new termolecular-kinetics model for CO₂ reaction with MEA solutions, which proved to be better than previously published kinetic models. The model was comprehensive enough to describe for the first time the absorption of CO₂ in highly concentrated and high CO₂-loaded aqueous MEA solutions for a wide temperature range.

© 2003 Elsevier Ltd. All rights reserved.

Keywords: Kinetics; Absorption; Numerical modeling; CO₂; MEA; Termolecular mechanism

1. Introduction

When designing or simulating an absorption column for CO₂ absorption associated with chemical reactions, certain key data are required. These key data include (a) physical, thermal, and transport properties of the gases and the liquids involved in the system, (b) vapor–liquid equilibrium data, (c) configuration data for the absorber internals, and (d) rate data for the chemical reactions. Early literature (Tontiwachwuthikul et al., 1992) indicated that it was not possible to simulate the behavior of packed columns using high CO₂-loaded aqueous MEA solution because fundamental data, such as the physical and chemical properties of the system as a function of CO₂ loading, were not available at that time. Also, it has been observed that absorption of CO₂ data into ultra-high concentrated MEA (i.e. ≥ 5 M) were absent (Versteeg et al., 1996) even though these are required for absorption column simulation and design. Furthermore, even though many physical properties such as density, viscosity, solubility, and diffusivity

of CO₂–MEA system have recently been published in the literature (Weiland et al., 1998; Tsai et al., 2000; Ko et al., 2001), these do not include the properties for the kinetics of high CO₂-loaded, concentrated aqueous MEA systems. It is well known that precise information on the reaction rate constants as well as a detailed knowledge of the reaction mechanism for the reaction between CO₂ and MEA solutions are essential for accurate design and simulation of the CO₂ absorption process.

Kinetic data of the reaction between CO₂ and aqueous MEA available in literature are summarized in Table 1. This table contains literature citations from the 1960s to the present, for various temperatures or temperature ranges of experiments, MEA concentrations or concentration ranges, and experimental techniques used to obtain the kinetic data. As well, this table shows that there are discrepancies between the values or expressions of the second order reaction-rate constants. In order to have a clearer picture for the discrepancies between these reaction-rate data, the data of the reaction-rate constants have been grouped based on the decades they were obtained and presented in Fig. 1. A closer look at these literature sources and the associated kinetic data show the following main points:

* Corresponding author. Tel.: +1-306-585-4160;
fax: +1-306-585-4855.

E-mail address: paitoon@uregina.ca (P. Tontiwachwuthikul).

Table 1
Literature data on the reaction between CO₂ and aqueous MEA

Reference	T (K)	[MEA] (mol/dm ³)	k (dm ³ /mol s)	Experimental Technique
Astarita (1961)	294.5	0.25–2.0	5400	Laminar jet absorber
Emmert and Pigrord (1962)	298	0.1–2.0	5400	Wetted wall column
Clarke (1964)	298	1.6–4.8	7500	Laminar jet absorber
Sharma (1965)	298	1.0	6970	Laminar jet absorber
Sharma (1965)	303	1.0	9700	Laminar jet absorber
Danckwerts and Sharma (1966)	291	1.0	5100	Laminar jet absorber
Danckwerts and Sharma (1966)	298	1.0	7600	Laminar jet absorber
Danckwerts and Sharma (1966)	308	1.0	13,000	Laminar jet absorber
Leder (1971)	353	—	90,400	Stirred cell reactor
Sada et al. (1976a)	298	0.2–1.9	7140	Laminar jet absorber
Sada et al. (1976b)	298	0.2–1.9	8400	Laminar jet absorber
Hikita et al. (1977, 1979)	278.6–308.4	0.02–0.18	$9.77 \times 10^{10} \exp(-4955/T)$	Rapid mixing method
Alvarez-Fuster et al. (1980)	293	0.2–2.0	4300	Wetted wall column
Donaldson and Nguyen (1980)	298	0.03–0.08	6000	Membranes method
Laddha and Danckwerts (1981)	298	0.49–1.71	5870	Stirred cell reactor
Penny and Ritter (1983)	278–303	0–0.06	$1.23 \times 10^{11} \exp(-5078/T)$	Stopped flow method
Sada et al. (1985)	303	0.5–2.0	7740	Stirred cell reactor
Barth et al. (1986)	293	0.02–0.05	3600	Stopped flow method
Barth et al. (1986)	298	0.02–0.05	4700	Stopped flow method
Crooks and Donnellan (1989)	298	0.02–0.06	3880	Stopped flow method
Alper (1990)	278–298	0–0.45	$8.51 \times 10^{11} \exp(-5617/T)$	Stopped flow method
Littel et al. (1992)	318	0–3.2	10,400	Stirred cell, numerical
Littel et al. (1992)	333	0–3.2	25,700	Stirred cell, numerical
Hagewiesche et al. (1995)	313	—	10,090	Laminar jet, numerical
Versteeg et al. (1996) ^a	Literature	Literature	$4.4 \times 10^{11} \exp(-5400/T)$	Literature Data
Xiao et al. (2000)	303	0.1–0.4	4774	Wetted wall column
Xiao et al. (2000)	308	0.1–0.4	7618	Wetted wall column
Xiao et al. (2000)	313	0.1–0.4	11,743	Wetted wall column
Hong and Li (2002)	303–313	0.1–0.5	$3.014 \times 10^{11} \exp(-5376.2/T)$	Wetted wall column

^aThe rate-constant expression is based on the published literature data up to 1992.

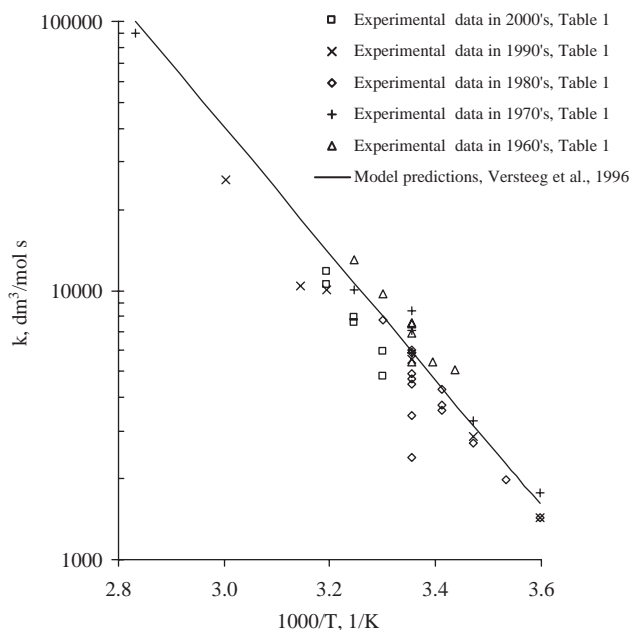


Fig. 1. Arrhenius plot for the reaction between CO₂ and aqueous MEA solutions (literature data).

First, despite the considerable number of studies, several disagreements exist between the published rate data. The reported values of the reaction rate constant (k) at 298 K vary from 3880 to 8400 dm³/mol s (see Table 1 and Fig. 1). The existence of this wide range of k can be attributed to (1) uncertainties in the physical properties used, (2) inability to determine the exact contact area between gas and liquid in the absorption process, (3) possibility of existence of interfacial turbulence in some types of absorbers, and (4) the assumption of a pseudo-first order reaction. In the case of problems associated with physical properties, examples include the work by Emmert and Pigrord (1962) and Sada et al. (1976a,b) who used the solubility and the diffusivity of CO₂ in water in their studies instead of properties for MEA solutions. On the other hand, Clarke (1964) conducted the experiments at a reduced pressure to avoid the depletion of unreacted MEA that was claimed to occur at the interface in their work. Examples in the case of interfacial turbulence include the work of Hikita et al. (1979) and Hagewiesche et al. (1995) who added a small amount of surface-active agents in order to reduce the values of the experimental absorption rates. The authors indicated that the higher absorption rates observed in the solution without surface active

agents may be attributed to interfacial turbulence, presumably produced by a surface tension gradient during the chemical absorption process, as observed by Brian et al. (1967), and also, reported by Sada et al. (1977). Finally, the assumption of pseudo-first order reactions used in most of the previous studies has been demonstrated by Littel et al. (1992) to give inaccurate kinetics.

Second, all of the data shown in Table 1 were obtained for experiments conducted at a single temperature, except for the four studies conducted by Hikita et al. (1977), Penny and Ritter (1983), Alper (1990), and Horng and Li (2002), where very narrow ranges of temperatures were covered. In the first three studies, the temperature range was 278–308 K, whereas in the fourth study the range of temperature was 303–313 K. It is well known that simple kinetic models cannot be extrapolated with confidence beyond the temperature and concentration ranges where their kinetic data were obtained. It is essential to mention that the kinetic data presented in the literature up to 1992 were compiled by Versteeg et al. (1996) and they derived an expression for the rate-constant as presented in Table 1. Although the published data of Leder (1971) and Littel et al. (1992) at temperatures above 313 K apparently appear to be consistent with the rate-constant expression of Versteeg et al. (1996) (see Table 1 and Fig. 1), these data were reported to be incorrect after a re-evaluation of the experimental data by Versteeg et al. (1996) who suggested that their rate-constant expression should be applied only up to a temperature of 313 K. Based on this work, it can be concluded that there are no accurate kinetic data above 313 K. This situation is mainly attributed to the limitation in experimental techniques available. Besides, the rate of reaction of CO₂ and MEA above 313 K is very fast and the reversibility of the reaction, which is required for the regeneration of the loaded amine solutions in gas treating processes, makes the interpretation both less simple and less straightforward (Versteeg et al., 1996).

Third, the concentration of MEA solutions used in previous experimental work did not exceed 2.0 mol/dm³, except for two studies conducted by Clarke (1964) and Littel et al. (1992), where the concentration reached 4.8 and 3.2 mol/dm³, respectively (see Table 1). In addition, the effect of CO₂ loading (a situation that exists in a commercial CO₂ absorption plant) on the kinetics was not taken into consideration in most of the literature data reported in Table 1. There are two ways to vary the free amine concentrations, either by varying the total amine concentration or the loading of CO₂ into solution. In the latter case, the effect of CO₂-loading on the physical properties is needed for the interpretation of the kinetics. Littel et al. (1992) questioned the kinetic data at high CO₂-loading that were reported by Savage and Kim (1985) because in their analysis the latter authors did not consider the CO₂-loading effects on the physical properties.

Fourth, only in two of the studies were the experimental data interpreted by utilizing numerically solved absorption models (Littel et al., 1992; Hagewiesche et al., 1995).

The other absorption studies mentioned in Table 1 were all analyzed by using the methodology of ‘gas absorption with pseudo first-order reaction’ and the related simplified form of penetration theory equations developed by Danckwerts (1970). However, the only way to obtain reliable kinetics reaction-rate data is by interpreting the experimental data with the aid of a numerically solved absorption model (Littel et al., 1992; Rinker et al., 1996; Versteeg et al., 1996).

The foregoing discussion therefore, suggests a strong need to obtain more accurate experimental data on a laboratory scale in order to clarify the kinetics of the present system. Such experimental work must take the following points into consideration. (1) Obtaining reliable data on the absorption rate of CO₂ into highly concentrated and partly CO₂-loaded MEA solutions under the condition of no interfacial turbulence. One of the best apparatus that can be used to generate reliable absorption data is the laminar jet absorber because the interfacial area is known accurately and the physical absorption rates have been shown to agree with penetration theory predictions (Danckwerts, 1970; Astarita et al., 1983). (2) Conducting the kinetics experiments within the typical range of temperature found in an industrial absorber, which is from 293 to 333 K. (3) Interpreting the experimental data with the aid of an efficient and effective numerically solved absorption model (Aboudheir et al., 2003) that takes into consideration all the possible reversible reactions of CO₂–MEA system. The actual physical and chemical properties of the system should be estimated as a function of temperature, MEA concentration, and CO₂-loading and then used in the interpretation of the absorption data. All these points constitute the objectives of this study. This paper will also use this comprehensive interpretation to develop a new expression for the kinetic constants in the rate model.

2. Theory

The theoretical absorption-rate model used to interpret the experimental kinetic data was developed based on all possible chemical reactions as well as the reaction mechanism. In order to solve this model numerically, the bulk concentrations, which are usually calculated by a vapor liquid equilibrium model (VLE), are required. Simply, developing the absorption-rate/kinetics model requires the reaction mechanism, vapor–liquid equilibrium model, and model parameters as given below.

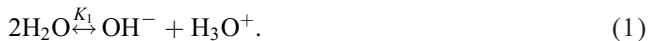
2.1. Reaction mechanism

The reactions between CO₂ and MEA solution have been described in the literature by two mechanisms; namely the zwitterion mechanism introduced by Danckwerts (1979) and the termolecular mechanism introduced by Crooks and Donnellan (1989). The zwitterion mechanism consists of the formation of a complex called a zwitterion, followed by the deprotonation of the zwitterion by a base (Danckwerts,

1979; Blauwhoff et al., 1984; Versteeg and van Swaaij, 1988; Littel et al., 1992).

Reactions 1–10 may occur when CO₂ absorbs into and reacts with aqueous MEA. All the species represented are in aqueous solution.

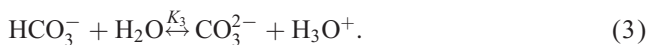
Ionization of water:



Dissociation of dissolved CO₂ through carbonic acid:



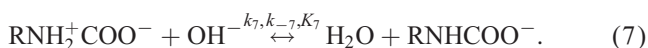
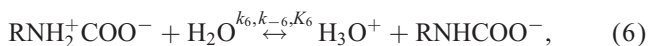
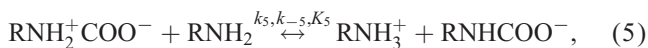
Dissociation of bicarbonate:



Zwitterion formation from MEA and CO₂ reaction:



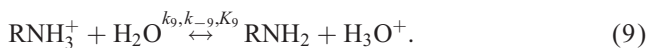
Carbamate formation by deprotonation of the zwitterion:



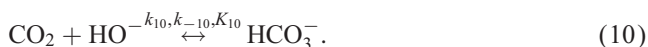
Carbamate reversion to bicarbonate (hydrolysis reaction):



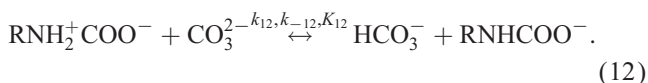
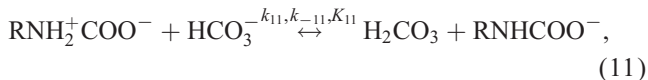
Dissociation of protonated MEA:



Bicarbonate formation:



Since CO₂-loaded aqueous MEA solutions were used in the experimental work, the concentrations of bicarbonates and carbonates in the aqueous solutions were considered significant. As such, the contributions of these species to the deprotonation of the zwitterion were investigated. As a result, additional reactions 11 and 12 became essential in describing the mechanism:



Based on this reaction scheme, the general rate of reaction of CO₂ with MEA via the zwitterion mechanism could be described as in Eq. (13) (Blauwhoff et al., 1984; Glasscock et al., 1991; Versteeg et al., 1996):

$$r_{\text{CO}_2\text{-MEA}} = \frac{[\text{CO}_2][\text{RNH}_2] - k_{-4}/k_4[\text{RNHCOO}^-](\sum k_{-b}[\text{BH}^+]/\sum k_b[\text{B}])}{1/k_4 + (k_{-4}/k_4 \sum k_b[\text{B}])}, \quad (13)$$

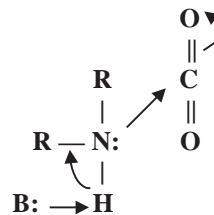


Fig. 2. Single step, termolecular reaction mechanism for the formation of carbamate according to Crooks and Donnellan (1989).

where B designates any species in the solution that can act as a base to abstract the proton from the zwitterion. In this case, the expected species for a loaded MEA solution are [RNH₂], [H₂O], [OH⁻], [HCO₃⁻], and [CO₃²⁻].

The termolecular mechanism assumes that the reaction is a single-step between CO₂ and MEA where the initial product is not a zwitterion but a loosely bound encounter complex with a mechanism of the type shown in Fig. 2. Most of these complexes are intermediates, which break up to give reagent molecules again, a few react with a second molecule of amine, or a water molecule, to give ionic products. Bond-formation and charge-separation occur only in the second step. The forward reaction rate for this mechanism is presented in Eq. (14) (Crooks and Donnellan, 1989; Versteeg et al., 1996).

$$r_{\text{CO}_2\text{-MEA}} = -(k_{\text{RNH}_2}[\text{RNH}_2] + k_{\text{H}_2\text{O}}[\text{H}_2\text{O}])[\text{RNH}_2][\text{CO}_2]. \quad (14)$$

In this work, we have used both mechanisms, zwitterion and termolecular, to evaluate the experimental kinetic data in an attempt to find an explanation for the relatively large scatter in the kinetic data presented in the literature (see Fig. 1 and Table 1). Regarding the reaction rate dependence on the CO₂ concentration, a first order rate equation was found in the literature (Blauwhoff et al., 1984). Therefore, only the reaction-rate dependence on MEA concentration and temperature will be considered in this research work. In addition, it should be mentioned that the temperature, concentration, and loading are operating variables for absorption at industrial scale. Therefore, the reversibility between the CO₂ and MEA, OH⁻, and H₂O cannot be ignored and was included in this kinetic study.

2.2. Vapor–liquid equilibrium model

Liquid bulk concentrations of all chemical species are required for kinetic analysis. A vapor–liquid equilibrium (VLE) model to estimate the CO₂ partial pressure and the liquid bulk concentrations of all the chemical species present in the solution was developed. The input data of the model

Table 2

Equilibrium constants used in the VLE model of this work. $\ln K = a_1/T + a_2 \ln T + a_3$

	a_1	a_2	a_3	T range (K)	Reference
K_1 , (mol/dm ³) ²	−13445.9	−22.4773	140.932	273–498	Edwards et al. (1978)
K_2 , (mol/dm ³)	−12092.1	−36.7816	235.482	273–498	Edwards et al. (1978)
K_3 , (mol/dm ³)	−12431.7	−35.4819	220.067	273–498	Edwards et al. (1978)
K_8 , (mol/dm ³)	−3090.83	0.0	6.69425	298–413	Kent and Eisenberg (1976)
K_9 , (mol/dm ³)	−5851.11	0.0	−3.3636	298–413	Kent and Eisenberg (1976)

include the initial concentration of the MEA solution, the initial CO₂ loading of the MEA solution, the equilibrium constants of the reactions, and the solubility of CO₂ into MEA solution. It has been assumed that all of the chemical reactions are at equilibrium. The concentration of water is assumed to remain constant because its concentration is much larger than the concentration of all other chemical species and also because of the short contact time in the laminar jet absorber. The concentrations for the remaining eight chemical species shown in the chemical reactions (see Section 2.1, reaction mechanism) were calculated by solving the mass balance equations and the Henry's law correlation, Eqs. (15)–(23).

MEA balance:

$$[\text{RNH}_2] + [\text{RNH}_3^+] + [\text{RNHCOO}^-] = [\text{MEA}]_0. \quad (15)$$

Carbon balance:

$$[\text{CO}_2] + [\text{HCO}_3^-] + [\text{CO}_3^{=}] + [\text{RNHCOO}^-] = \alpha[\text{MEA}]_0. \quad (16)$$

Charge balance:

$$[\text{RNH}_3^+] + [\text{H}_3\text{O}^+] = [\text{HCO}_3^-] + [\text{OH}^-] + 2[\text{CO}_3^{=}] + [\text{RNHCOO}^-]. \quad (17)$$

Independent equilibrium constants:

$$K_1 = [\text{OH}^-][\text{H}_3\text{O}^+], \quad (18)$$

$$K_2 = [\text{HCO}_3^-][\text{H}_3\text{O}^+]/[\text{CO}_2], \quad (19)$$

$$K_3 = [\text{CO}^{=}][\text{H}_3\text{O}^+]/[\text{HCO}_3^-], \quad (20)$$

$$K_8 = [\text{RNH}_2][\text{HCO}_3^-]/[\text{RNHCOO}^-], \quad (21)$$

$$K_9 = [\text{RNH}_2][\text{H}_3\text{O}^+]/[\text{RNH}_3^+]. \quad (22)$$

In addition to these mass balance equations, the Henry's law relationship between the equilibrium partial pressure and the free concentration of CO₂ is required:

$$P_{\text{CO}_2} = He \times [\text{CO}_2]. \quad (23)$$

In order to solve these nonlinear algebraic equations for the bulk concentrations and the equilibrium partial pressure, the values of the solubility (in terms of Henry's law constant, He) and the equilibrium constants are required. The solubility of CO₂ in amine was calculated using the N₂O analogy. Details of the calculation are based on the work of Wang

et al. (1992) and Tsai et al. (2000). The equilibrium-constants K_1 , K_2 , K_3 , shown in Table 2, were calculated by the correlations developed by Edwards et al. (1978). These correlations are well established and have been utilized in many VLE models such as the Austgen et al. model (1989) and the Li–Mather model (1994). The equilibrium constants K_8 and K_9 , can be calculated from simple correlations developed by Kent and Eisenberg (1976) (see Table 2).

The nine nonlinear algebraic equations, Eqs. (15)–(23), were solved for the nine unknowns of the bulk concentrations and the equilibrium partial pressure using a subroutine called DNEQNF documented in the IMSL MATH/Library (Visual Numerics, Inc., 1994a) for solving a system of nonlinear algebraic equations. This routine is based on the MINPACK subroutine HYBRD1, which uses a modification of M.J.D. Powell's hybrid algorithm. The algorithm is a variation of Newton's method, which uses a finite-difference approximation to the Jacobian and takes precautions to avoid large step sizes or increasing residuals (More et al., 1980; (Visual Numerics, Inc., 1994a)). As a finite-difference method is used to estimate the Jacobian, double precision calculation was applied in order to get an accurate Jacobian, which will assist in arriving at the exact roots of the equations. Using this technique, it has been found that the program converged to the solution even when the initial guesses of the bulk concentrations and the partial pressure were not close to the solution.

Fig. 3 shows a comparison between the results calculated by the VLE model of this work and published experimental data. The experimental VLE data of MEA–CO₂–H₂O system reported in this figure are the most frequently used data in the literature to test both the VLE apparatus and VLE models. At CO₂ loading of less than 0.6, a good agreement between the model predictions and the experimental VLE data was obtained by using the K_8 and K_9 correlations of Kent and Eisenberg (1976). Since in industrial processes, lean CO₂ loading ranges from about 0.1 to 0.2 and rich CO₂ loading from about 0.3 to 0.55, the K_8 and K_9 correlations developed by Kent and Eisenberg (1976) were selected and incorporated in the VLE model. At loading values of less than 0.55 (the industrial loading range), the average absolute deviation between the predicted and experimental VLE data was found to be 12.5%. Typical range of uncertainty in VLE data for CO₂–MEA system is 20% (Austgen et al., 1989). It should be mentioned that the non-ideality

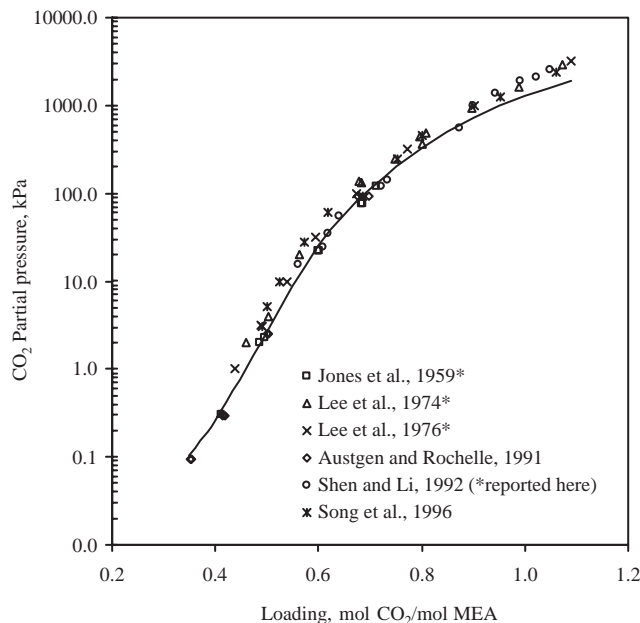


Fig. 3. Carbon dioxide equilibrium partial pressure over a 2.5M MEA solution at 313 K. Points are experimental data. Solid line is predicted by using K_8 and K_9 of Kent and Eisenberg (1976). (See references: Austgen and Rochelle, 1991; Shen and Li, 1992; and Song et al. 1996).

of the system was accounted for and was lumped into the correlations of K_8 and K_9 . With this accuracy and the computational simplicity, there was no need to use the more rigorous VLE models such as Deshmukh–Mather model (1981) or Austgen et al. model (1989) in this work.

Some results for the bulk concentrations obtained by the VLE model are shown in Fig. 4. This figure shows how the speciation–concentration plots from this work have a trend similar to those obtained by Austgen et al. (1989) and Liu et al. (1999) using the Electrolyte-NRTL model for presenting vapor–liquid–equilibria in acid gas–alkanolamine–water system. As shown in Fig. 4, the main products with high concentration are $[\text{RNH}_3^+]$, $[\text{HCO}_3^-]$, and $[\text{RNHCOO}^-]$ when the loading is less than 0.5. At a loading of 0.5, further CO_2 absorption causes carbamate reversion to bicarbonate, $[\text{HCO}_3^-]$. When additional carbon dioxide is absorbed into a highly loaded MEA solution, the liquid bulk concentration of free carbon dioxide, $[\text{CO}_2]$, is increased and is not negligible compared to its interfacial concentration. As a result, it has been recommended to use the free concentration of $[\text{CO}_2]$ in the calculation of the enhancement factor and the absorption rates of CO_2 into loaded aqueous MEA. This recommendation was implemented in this work.

2.3. Absorption-rate/kinetics model

A comprehensive absorption-rate/kinetics model was developed for interpreting the absorption data of CO_2 into

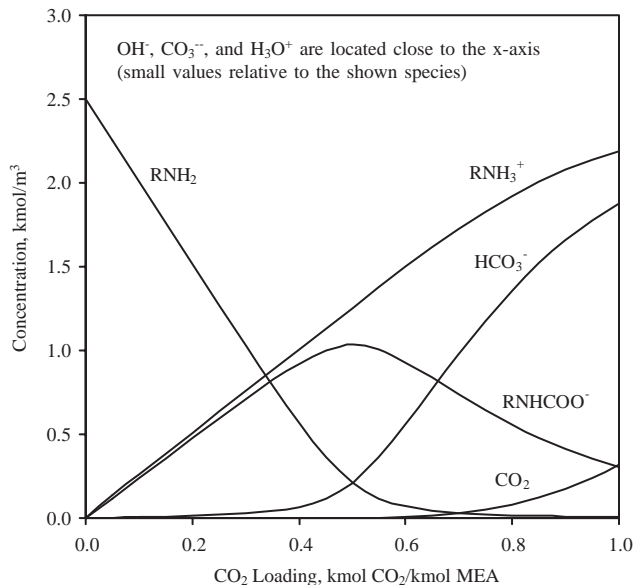


Fig. 4. Liquid-phase speciation and concentration in 2.5M MEA solution with CO_2 loading from 0 to 1 at 313 K. Compositions were predicted by the VLE model developed in this work.

MEA solutions, from which the kinetics data were extracted. The model takes into account the coupling between chemical equilibrium, mass transfer, and chemical kinetics of all possible chemical reactions. The mathematical model is capable of predicting gas absorption rates and enhancement factors from the system hydrodynamics and the physico-chemical properties, as well as predicting the kinetics of reaction from experimental absorption data. A rigorous numerical method to solve the system of unsteady-state partial differential equations was developed. The numerical scheme employed utilizes the Barakat–Clark method (Barakat and Clark, 1966) for solving diffusive differential equations. This explicit finite difference scheme was found to be very suitable because it is unconditionally stable and gives accurate predictions for concentration profiles as well as for absorption rates of gas into liquid. The model was validated by comparing its predictions with the experimental data of CO_2 absorption into water and MEA solutions, as well as N_2O absorption into MEA solutions (Aboudheir et al., 2003). In brief, the diffusion equation in Eq. (24) is the one most frequently used to represent the absorption of gas into liquid jets. This equation, Eq. (24), governs the variation in time and space of the concentration of the reactants and the products in the liquid phase (one equation for each component or material balance).

$$D_j \frac{\partial^2 C_j}{\partial x^2} = \frac{\partial C_j}{\partial t} + r_i \quad (24)$$

The chemical species in reactions 1–12 have been renamed for convenience in the numerical treatment as follows: $C_1 = [\text{CO}_2]$, $C_2 = [\text{RNH}_2]$, $C_3 = [\text{RNH}_3^+]$, $C_4 = [\text{HCO}_3^-]$, $C_5 = [\text{OH}^-]$, $C_6 = [\text{CO}_3^{2-}]$, $C_7 = [\text{H}_3\text{O}^+]$, $C_8 = [\text{RNHCOO}^-]$, and $C_9 = [\text{H}_2\text{O}]$.

Eqs. (25)–(29), which are based on Eq. (24), represent the diffusion of the gas accompanied with reaction into the liquid near the interface:

CO₂ reaction balance:

$$\frac{\partial C_1}{\partial t} = D_1 \frac{\partial^2 C_1}{\partial x^2} + r_2 + r_{\text{CO}_2\text{-MEA}} + r_{10}. \quad (25)$$

The total CO₂ balance:

$$\begin{aligned} \frac{\partial C_1}{\partial t} + \frac{\partial C_4}{\partial t} + \frac{\partial C_6}{\partial t} + \frac{\partial C_8}{\partial t} \\ = D_1 \frac{\partial^2 C_1}{\partial x^2} + D_4 \frac{\partial^2 C_4}{\partial x^2} + D_6 \frac{\partial^2 C_6}{\partial x^2} + D_8 \frac{\partial^2 C_8}{\partial x^2}. \end{aligned} \quad (26)$$

Total MEA balance:

$$\frac{\partial C_2}{\partial t} + \frac{\partial C_3}{\partial t} + \frac{\partial C_8}{\partial t} = D_2 \frac{\partial^2 C_2}{\partial x^2} + D_3 \frac{\partial^2 C_3}{\partial x^2} + D_8 \frac{\partial^2 C_8}{\partial x^2}. \quad (27)$$

Charge balance:

$$\begin{aligned} \frac{\partial C_3}{\partial t} + \frac{\partial C_7}{\partial t} - \frac{\partial C_4}{\partial t} - \frac{\partial C_5}{\partial t} - 2 \frac{\partial C_6}{\partial t} - \frac{\partial C_8}{\partial t} \\ = D_3 \frac{\partial^2 C_3}{\partial x^2} + D_7 \frac{\partial^2 C_7}{\partial x^2} - D_4 \frac{\partial^2 C_4}{\partial x^2} - D_5 \frac{\partial^2 C_5}{\partial x^2} \\ - 2D_6 \frac{\partial^2 C_6}{\partial x^2} - D_8 \frac{\partial^2 C_8}{\partial x^2}. \end{aligned} \quad (28)$$

Carbamate balance:

$$\frac{\partial C_8}{\partial t} = D_8 \frac{\partial^2 C_8}{\partial x^2} + r_8 - r_{\text{CO}_2\text{-MEA}}. \quad (29)$$

Equilibrium instantaneous reactions:

In order to eliminate the likelihood of using very large reaction rates for the instantaneous reactions (reactions 1, 3, and 9) from the model equations, their equilibrium constant expressions were used to complete the model equations for concentration profile calculations. These equilibrium constant expressions are given below in Eqs. (30)–(32).

$$K_1 = C_5 C_7, \quad (30)$$

$$K_3 = \frac{C_6 C_7}{C_4}, \quad (31)$$

$$K_9 = \frac{C_2 C_7}{C_3}. \quad (32)$$

The above eight equations (Eqs. (25)–(32)) were solved for the concentration profiles of the eight chemical species, C_1, C_2, \dots, C_8 , subject to the initial and boundary conditions given in Eqs. (33)–(36).

Initial conditions:

for all chemical species, $j = 1, 2, \dots, 8$.

$$C_j(x, 0) = C_j^0 \quad \text{at } t = 0 \text{ and } 0 \leq x \leq \infty. \quad (33)$$

Boundary conditions:

for all chemical species, $j = 1, 2, \dots, 8$.

$$C_j(\infty, t) = C_j^0 \quad \text{at } x = \infty \text{ and } 0 \leq t \leq \tau \quad (34)$$

for all volatile chemical species, $j = 1$.

$$C_j(0, t) = C_j^* = \frac{P_j}{H e_j} \quad \text{at } x = 0 \text{ and } 0 \leq t \leq \tau \quad (35)$$

for all non-volatile chemical species, $j = 2, 3, \dots, 8$.

$$\frac{dC_j}{dx}(0, t) = 0 \quad \text{at } x = 0 \text{ and } 0 \leq t \leq \tau. \quad (36)$$

Using the obtained concentration profile data of the absorbed gas, C_1 , the local absorption rate per unit area was calculated using Eq. (37).

$$N = -D_1 \left(\frac{\partial C_1}{\partial x} \right)_{x=0}. \quad (37)$$

The term $(\partial C_1 / \partial x)_{x=0}$ is the concentration gradient at the surface and it is a function of time. The average absorption rate per unit area of solute gas by the liquid jet of length h is obtained by integrating Eq. (37) over the contact time as shown in Eq. (38) (Astarita, 1967; Danckwerts, 1970).

$$N_{\text{ave}} = -\frac{D_1}{\tau} \int_0^\tau \frac{\partial C_1}{\partial x}(0, t) dt. \quad (38)$$

Details of the numerical implementation of this absorption-rate model are documented elsewhere (Aboudheir et al., 2003).

When the dissolved gas reacts with the liquid, it is often convenient to present the effect of a chemical reaction in terms of the enhancement factor, E , defined as the ratio of the absorption rate of a gas into a reacting liquid to that if there was no reaction, as given in Eq. (39).

$$E = \frac{N_{\text{ave}}}{k_L^0 (C^* - C^0)}, \quad (39)$$

N_{ave} was obtained from Eq. (38) whereas k_L^0 was evaluated from $k_L^0 = 4/d\pi\sqrt{DL}/h$, an expression that is valid in the case of laminar jet absorber (Danckwerts, 1970; Astarita et al., 1983).

Numerical calculation of the kinetics of the reaction is usually achieved by interpreting experimental-absorption rate data with the aid of a numerically solved absorption-rate model such as the one presented above. For each absorption rate experiment, the predicted enhancement factor (E_{pred}) is fitted to the experimentally observed enhancement factor (E_{exp}), with the apparent reaction-rate constant (k_{app}) as an adjustable parameter. In this work, the root finding algorithm of Muller's method (entitled ZREAL) as documented in the IMSL MATH/Library (Visual Numerics Inc., 1994a) was used to find the zero of the real function according to Eq. (40).

$$f(k_{\text{app}}) = E_{\text{exp}} - E_{\text{pred}}. \quad (40)$$

Then the experimental apparent reaction-rate constants (k_{app}) obtained at one temperature but at different operating conditions (concentration, loading, and contact time) were fitted to the reaction rate expression in Eq. (41) for termolecular mechanism and in Eq. (45) for the zwitterion mechanism.

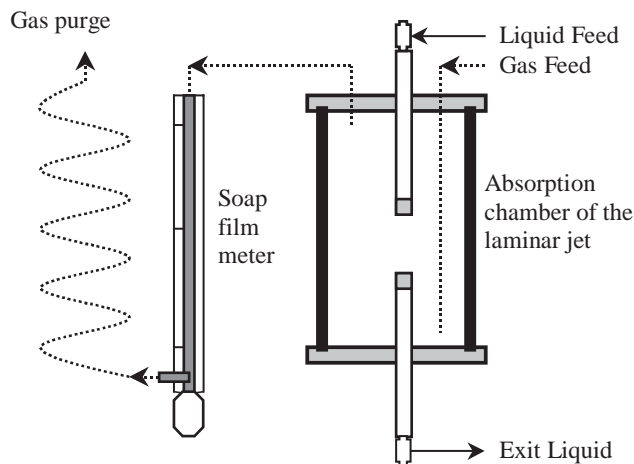


Fig. 5. Schematic drawing of laminar jet apparatus.

2.4. Model parameters

The calculation of the concentration profiles using the absorption rate model presented in this work requires knowledge of the physico-chemical properties of the fluids involved in the absorption process. These include density, viscosity, solubility, diffusivity, and reaction rate constants.

The density and viscosity of aqueous MEA solution were calculated according to the correlations developed by Weiland et al. (1998). The N_2O analogy was used to determine the solubility and diffusivity of CO_2 in amine solutions. The solubility of N_2O in amine solutions was calculated from a semi-empirical model of the excess Henry's constant proposed by Wang et al. (1992). The enhanced parameters for this semi-empirical model by Tsai et al. (2000) were adapted in this work. The diffusivity of N_2O in MEA was calculated from the simple correlation developed by Ko et al. (2001). On the other hand, the diffusivity of MEA in the aqueous MEA solutions was calculated from the correlation developed by Snijder et al. (1993). The forward rate coefficients of CO_2 reaction with water and hydroxide (k_2 and k_{10}) were calculated from the correlations reported by Pinsent et al. (1956). Each physical and chemical property was programmed in a Fortran-90 subroutine within a computer module, where it could be called and utilized as required.

3. Experimental work

A laminar jet apparatus was used to generate kinetics data for the absorption of CO_2 into high CO_2 -loaded and concentrated solutions of MEA. Fig. 5 shows the schematic drawing of the laminar jet apparatus used in this work. For each test run, the absorbing liquid was prepared and degassed by spraying it into a vacuum. A jet of the liquid issuing from a circular nozzle flowed intact downward through an atmosphere of the absorbed gas, and was collected in a capillary

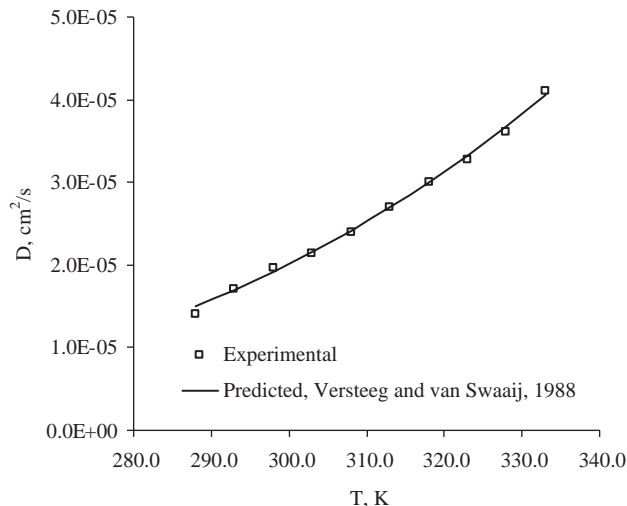


Fig. 6. Diffusivity of CO_2 into water as a function of temperature.

receiver. The nozzle, a circular hole in a 0.07 ± 0.005 mm thick stainless-steel sheet, was 0.63 mm in inside diameter. The receiver was a capillary-hole drilled in an acrylic rod. The length and the diameter of the hole were 2.0 and 0.1 cm, respectively. A two-dimensional traveling microscope was used to measure the jet-length to within one hundredth of a millimeter and the jet-diameter to within one thousandth of a millimeter. The actual flow rate of liquid was determined by weighing the liquid discharged in a timed interval during each experiment. A volumetric technique, recommended and used by other authors (Astarita, 1961; Al-Ghawaz et al., 1989; Rinker et al., 1996), was used to measure the absorption rates of gas into liquid. The used flow meter (digital soap-film meter) to measure the absorption rate was designed to measure flows from 0.1 to 50 cm^3/min with an accuracy of $\pm 3\%$ of readings. The temperatures of the liquid entering and leaving the jet chamber, of the gas entering the jet chamber, and of the gas entering the gas-flow-meter were measured. The temperatures of the liquid and the gas entering the jet chamber were controlled to within $\pm 0.3^\circ C$. This was achieved by having two separate heating/cooling circulator units, one for controlling the gas-stream temperature and the other for controlling the liquid-stream temperature. The absorption experiments at predetermined operating conditions were repeated several times and an average was taken for the absorption data.

The behavior of the laminar jet absorber was tested as a function of temperature by calculating experimentally the temperature effect on the diffusivity of CO_2 in water within the temperature range from 288 to 333 K, the typical temperature range found in gas absorbers. Fig. 6 shows this experimental diffusivity as well as the predicted diffusivity from the model developed by Versteeg and van Swaaij (1988). The results showed that excellent agreement between the measured and predicted diffusivity was obtained. The average absolute deviation of the measured diffusivity from the

predicted diffusivity is 1.7%. This indicates that the behavior of the laminar jet is excellent within this temperature range, the same temperature range for the planned experiments to produce the kinetic data of this work.

The experimental kinetic data for the present study were obtained by absorption of CO_2 into aqueous MEA solutions. The total MEA concentrations were in the range from 3.0 to 9.0 mol/dm³ and the total CO_2 -loading in solution ranged from ~ 0.1 to 0.49 mol CO_2 /mol MEA. All the kinetic experiments were conducted at atmospheric pressure and at temperatures in the range from 293 to 333 K. The raw experimental absorption data and kinetic data, in tabular forms, are documented elsewhere (Aboudheir, 2002, Appendix F, 15 pp.).

4. Results and discussion

All experimental absorption rate data obtained in the laminar jet absorber were interpreted by means of a numerically solved absorption-rate/kinetics model presented in this work. For each absorption rate data obtained, the calculated enhancement factor was fitted to the experimentally observed enhancement factor with the apparent reaction-rate constant (k_{app}) as an adjustable parameter. The experimental results of these k_{app} constants are presented in Fig. 7. A definite temperature dependence of the overall reaction rate can be observed for the five temperatures studied (293, 303, 313, 323, and 333 K). Applying regression analysis on the obtained data of the highly loaded and concentrated MEA solutions, the k_{app} constants showed that the order of reaction ranged from 1.2 to 1.5 within the temperature range 293–333 K. This behavior is different from the first-order behavior in the low MEA concentrations reported in the previous literature (see Table 1).

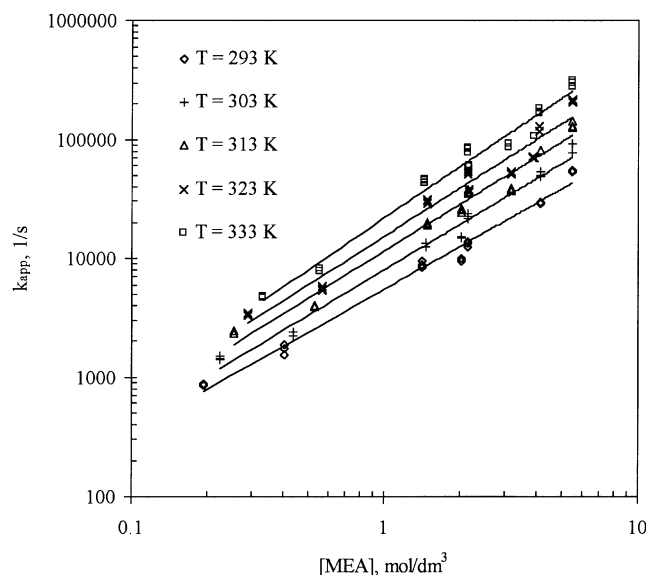


Fig. 7. Experimental results of the apparent reaction-rate constants for CO_2 reaction with MEA solutions.

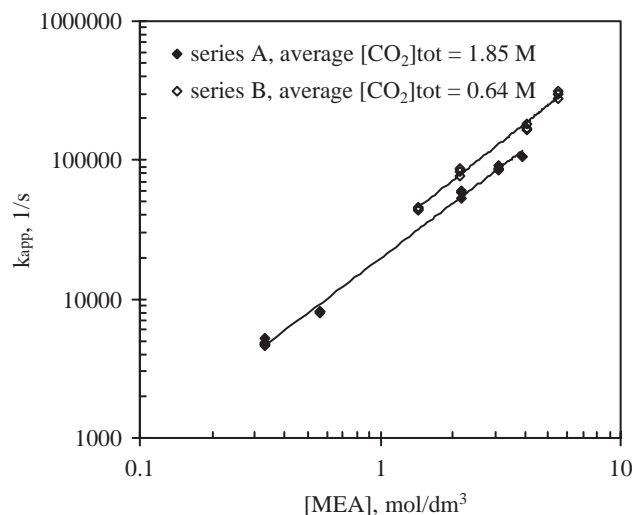


Fig. 8. Experimental results of the apparent reaction rate constants for CO_2 -MEA at 333 K.

In order to have a clearer picture for this behavior, the above kinetic data were classified and rearranged into two classes. Series-A is the low concentration data and series-B is the high concentration data. The concentration of free MEA, $[\text{RNH}_2]$, in series-A data ranges from 0.193 to 3.879 mol/dm³ with an average CO_2 loading, $[\text{CO}_2]_{\text{tot}}$, of 1.8 mol/dm³. On the other hand, the $[\text{RNH}_2]$ in series-B data ranges from 1.405 to 5.498 mol/dm³ with an average $[\text{CO}_2]_{\text{tot}}$ of 0.6 mol/dm³. Fig. 8 represents the new look of the kinetics data at 333 K, as an example. Similar figures were obtained for the other experimental temperatures, 293, 303, 313, and 323 K. Applying regression analysis on the data represented in these figures gave the orders of reaction and the reaction rate constant at each temperature and concentration series, as shown in Table 3. A close look at Fig. 8 and Table 3 shows four important observations.

First, the kinetics data obtained for low MEA concentration, series-A, and within the temperature range of 293–313 K (the gray region in Table 3) are in agreement with the literature kinetics data of Table 1. For example, the order of reaction can be approximated to one and the reaction rate constants are in agreement with the experimental literature data within these low temperature and concentration ranges. This indicates that the laminar jet apparatus is well designed, the measured kinetics data are accurate, and the absorption rate/kinetics model utilized in this work is accurate and efficient.

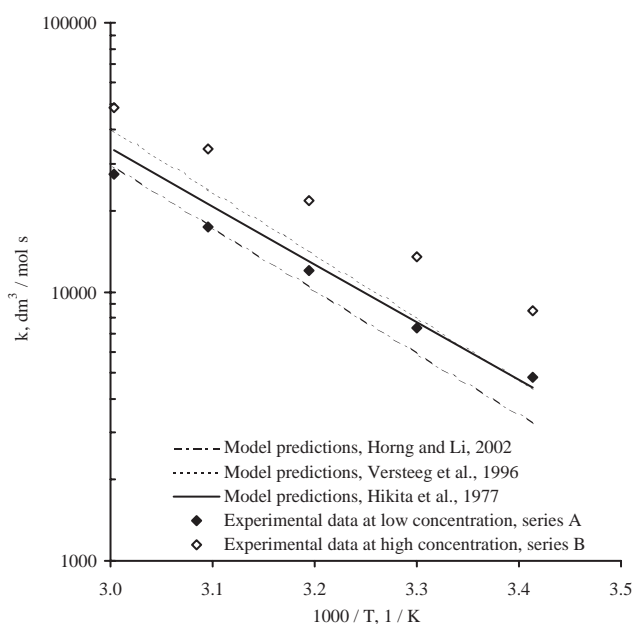
Second, the apparent rate constant decreases with increasing CO_2 -loading in the liquid as shown in Fig. 8. This can be explained on the basis of decreases in the free MEA and hydroxyl ions concentrations with increasing CO_2 -loading in the solution.

Third, the apparent reaction order in amine increases with increasing MEA concentration and temperature (see Table 3). This may be another indication that the reaction

Table 3

Apparent reaction order and second-order rate constant for CO₂ absorption into MEA solutions, when assuming $r = k_{\text{app}}[\text{CO}_2]$ and $k_{\text{app}} = k[\text{MEA}]^n$

$T(K)$	Series A: $[\text{CO}_2]_{\text{tot}} \sim 1.8 \text{ mol/dm}^3$ and $[\text{MEA}] = 0.193\text{--}3.879 \text{ mol/dm}^3$		Series B: $[\text{CO}_2]_{\text{tot}} \sim 0.6 \text{ mol/dm}^3$ and $[\text{MEA}] = 1.405\text{--}5.498 \text{ mol/dm}^3$	
	n (reaction order)	k ($\text{dm}^3/\text{mol s}$)	n (reaction order)	k ($\text{dm}^3/\text{mol s}$)
293	1.04	4615	1.29	5338
303	1.08	6674	1.37	7691
313	1.16	10,119	1.42	11,643
323	1.21	13,479	1.45	17,141
333	1.31	19,635	1.36	27,706

Fig. 9. Arrhenius plot for the reaction between CO₂ and aqueous MEA solutions by assuming $r = k_{\text{app}}[\text{CO}_2]$ and $k_{\text{app}} = k[\text{MEA}]^n$, where $n = 1$.

rate increases based on the presence of increasing amounts of free MEA while temperature effects appear to be typical of Arrhenius behavior. Fourth, if the simple kinetics model $r = k[\text{MEA}][\text{CO}_2]$ is assumed for all the measured kinetic data of this work, then the kinetic data of this work as well as those estimated from three models are as presented in Fig. 9. The first of these three models selected for evaluation was developed by Hikita et al. (1977), and is the most frequently referenced model in the literature. The second model was developed by Versteeg et al. (1996), and based on the kinetics data presented in the literature up to the year 1992. The third model was developed by Horn and Li (2002), and is the most recently published model in literature. As shown in Fig. 9, there is a close agreement for low concentrations (series-A data) and a deviation at high concentrations (series-B data) when compared with the three published kinetics models. This suggests that the reaction mechanism is either not as simple or as intrinsic as it appears. Thus, the behavior calls for more complicated

kinetic models in order to explain these results, especially at high CO₂-loaded and concentrated MEA solutions and elevated temperatures. This complex behavior led Versteeg et al. (1996) to place a temperature constraint, maximum of 313 K, on the applicability of their kinetics model, although their model was based on all published kinetics data for many decades and over wide ranges of concentrations and temperatures (see Table 1).

Based on this observation, a more comprehensive kinetics model for the reaction of CO₂ with MEA solutions is required in order to empirically predict the correct behavior of CO₂ absorption into highly loaded and concentrated MEA solutions. The experimental apparent reaction-rate-constants obtained in this work were critically analyzed by the two reaction-mechanisms reported in the literature, the termolecular mechanism and the zwitterion mechanism.

4.1. Kinetics of reaction according to the termolecular reaction mechanism

The apparent reaction rate expression of the termolecular mechanism can be presented by Eq. (41), which was derived from Eq. (14).

$$k_{\text{app}} = k_{\text{RNH}_2}[\text{RNH}_2]^2 + k_{\text{H}_2\text{O}}[\text{H}_2\text{O}][\text{RNH}_2]. \quad (41)$$

All the experimental k_{app} constants obtained from the absorption-rate/kinetics model were fitted to this termolecular mechanism expression, Eq. (41). A multiple linear regression procedure was applied to find the fitting parameters at each temperature. The subroutine called RLSE documented in the IMSL STAT/library (Visual Numerics Inc., 1994b) was used to obtain the optimum fitting parameters. In this way, the values of k_{RNH_2} and $k_{\text{H}_2\text{O}}$ were obtained. These are presented in Table 4. The absolute average deviation between the experiments and the fitted model are shown for each temperature, which indicates that all the experimental kinetics data of this work are fitted with an average absolute deviation (AAD%) of less than 16% by the rate constants reported in Table 4. A linear regression analysis for these data gave the kinetics expressions of Eqs. (42) and (43) based on the termolecular reaction mechanism.

$$k_{\text{RNH}_2} = 4.61 \times 10^9 \exp\left(\frac{-4412}{T}\right), \quad (42)$$

Table 4

Fitted values of kinetics constants of CO₂ absorption into MEA solution based on the termolecular reaction mechanism

Temperature (K)	293	303	313	323	333
k_{RNH_2} , dm ⁶ /mol ² s	1372.0	2021.7	3541.8	5784.2	7766.9
$k_{\text{H}_2\text{O}}$, dm ⁶ /mol ² s	56.3	108.7	129.7	122.1	287.1
AAD% in k_{app}	16.8	9.4	12.6	22.3	15.5

Table 5

Kinetics data at 298 K for CO₂ absorption into MEA solution based on the termolecular reaction mechanism

Reference	k_{RNH_2} (dm ⁶ /mol ² s)	$k_{\text{H}_2\text{O}}$ (dm ⁶ /mol ² s)
Crooks and Donnellan (1989)	52,600	24
This work, Eqs. (6.4) and (6.5)	1713.2	73.7

$$k_{\text{H}_2\text{O}} = 4.55 \times 10^6 \exp\left(\frac{-3287}{T}\right). \quad (43)$$

Based on the termolecular mechanism and the reaction-rate constant parameters found in this work (Eqs. (42) and (43)), the reversible reaction rate for CO₂ absorption into MEA solutions can be presented as in Eq. (44).

$$r_{\text{CO}_2\text{-MEA}}$$

$$= - (k_{\text{RNH}_2}[\text{RNH}_2] + k_{\text{H}_2\text{O}}[\text{H}_2\text{O}]) \times \left([\text{RNH}_2][\text{CO}_2] + \frac{1}{K_{\text{RNH}_2}} [\text{RNHCOO}^-][\text{H}_3\text{O}^+] \right), \quad (44)$$

where K_{RNH_2} (in dimensionless units) is the equilibrium constant of the carbamate formation reaction (sum of reactions 4, 5, and 9), which can be obtained by the correlation given by Barth et al. (1986). The concentrations of the chemical species (in mol/dm³) can be calculated from the VLE model presented in this work. Table 5 shows the values of the kinetic constants at 298 K obtained in this work (calculated by Eqs. (42) and (43)) and those obtained by Crooks and Donnellan (1989). To our knowledge, these are the only set of kinetic data published in the literature according to the termolecular mechanism. The data in this table are not comparable and it is believed that the data reported by Crooks and Donnellan (1989) are not correct for two reasons: First, no agreement was found between their experimental k_{app} data and the published data by Hikita et al. (1979) and Laddha and Danckwerts (1981) as shown in Fig. 10. By applying regression analysis on these low concentration data, the k_{app} data of Crooks and Donnellan (1989) showed that the order of reaction in terms of MEA concentration was 1.6. This is in contradiction with the unity order that has been reported in the past literature within this low concentration range and at 298 K (see Table 1). Second, the Crooks–Donnellan's model and its reaction-rate parameters could

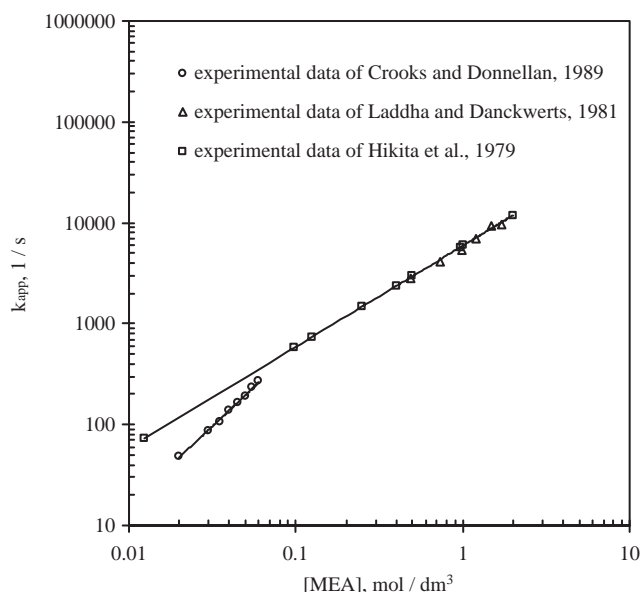


Fig. 10. Experimental results of the apparent reaction-rate constants for CO₂ reaction with low MEA concentrations at 298 K (literature data).

not predict the experimental apparent reaction-rate constant data reported in the literature at 298 K, as shown in Fig. 11. On the other hand, these experimental data are in good agreement with those predicted by using the kinetic equations developed in this work.

The measured k_{app} by Hikita et al. (1979) are compared in the parity plot shown in Fig. 12 with the predicted k_{app} by the termolecular-kinetics model of this work. A good agreement between the measured and predicted k_{app} for loaded and unloaded MEA solutions was obtained. The AAD% of the measured k_{app} from the predicted k_{app} was 19.4% for the unloaded solutions. This deviation increased slightly to 25.6% for the loaded MEA solutions. It should be mentioned that the solubility figures used by Hikita et al. (1979) were incorrect as reported by Laddha and Danckwerts (1981). This may explain the high deviations between the measured and predicted k_{app} .

When more accurate measurements of k_{app} (kinetics data of Laddha and Danckwerts, 1981) are compared with the predicted k_{app} by the kinetic model of this work, an excellent agreement between the measured and predicted k_{app} were obtained as shown in Fig. 13. The AAD% of the measured k_{app} from the predicted k_{app} is 7.8%. Based on these results, it can be stated that the developed kinetics model

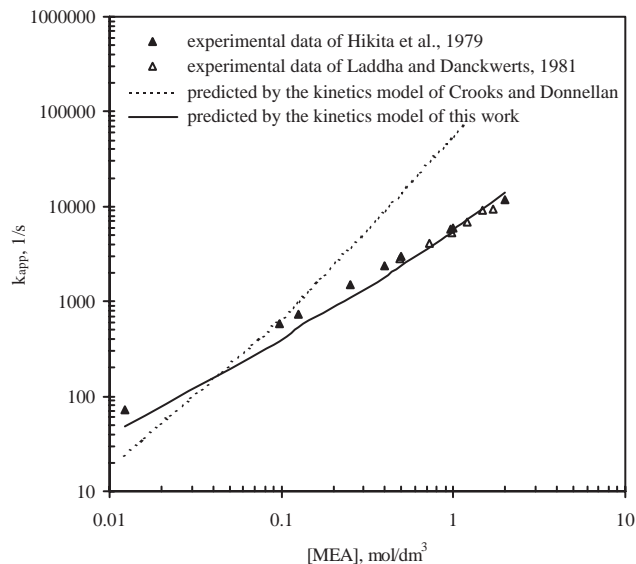


Fig. 11. Experimental and predicted apparent reaction-rate constants for CO_2 reaction with MEA solutions at 298 K.

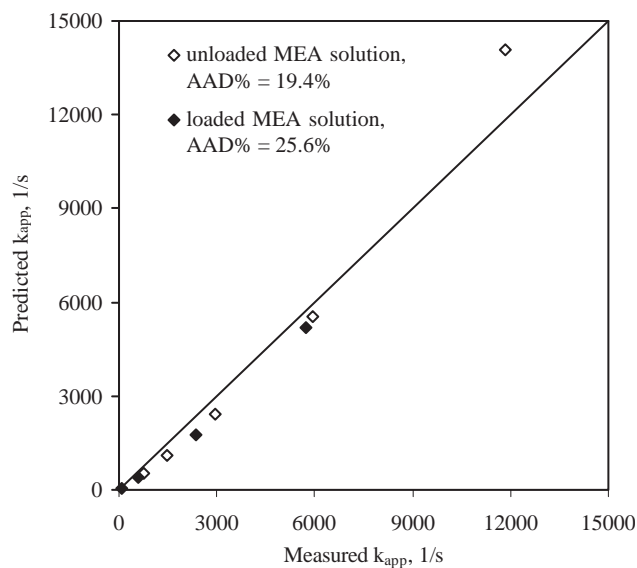


Fig. 12. Comparison of measured and predicted apparent reaction-rate constants of CO_2 -MEA system at 298 K. Measured data by Hikita et al. (1979) and predicted data by the termolecular-kinetics model of this work.

gave accurate representations for CO_2 -MEA system at low concentrations (within the free MEA concentration range of 0.01–2.00 mol/dm³).

In order to study the effectiveness of the termolecular-kinetics model developed in this work for CO_2 absorption into highly loaded and concentrated MEA solutions, the termolecular-kinetics model was integrated with the absorption-rate model and the enhancement-factors were predicted by Eq. (39). The ratios of the predicted enhancement factor to the experimental enhancement factor, E_R ,

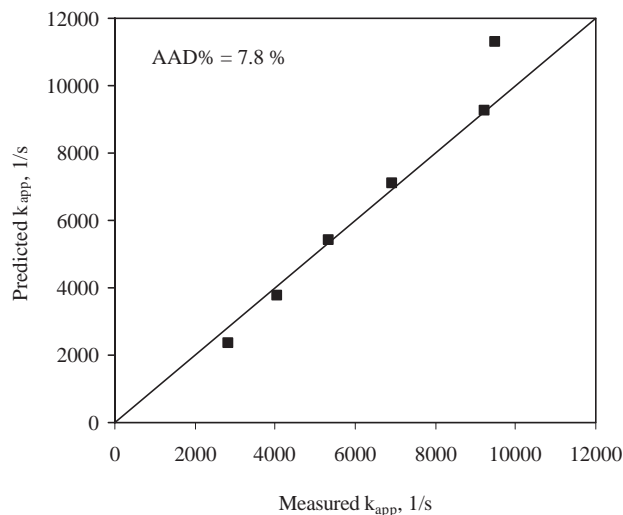


Fig. 13. Comparison of measured and predicted apparent reaction-rate constants of CO_2 -MEA system at 298 K. Measured data by Laddha and Danckwerts (1981) and predicted data by the termolecular-kinetics model of this work.

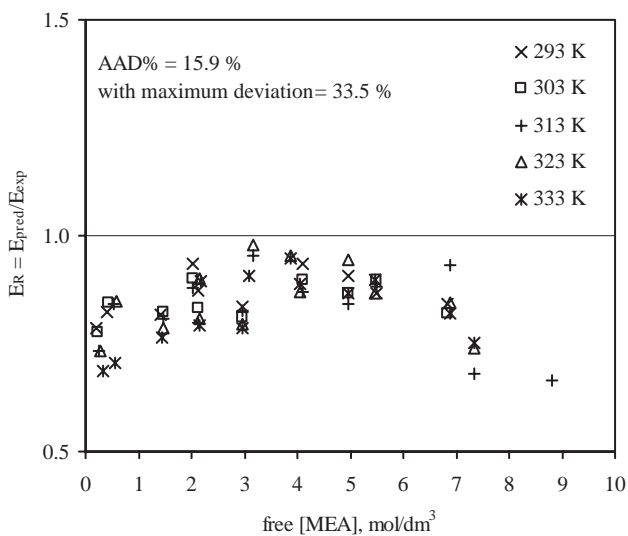


Fig. 14. Influence of the free MEA concentration on the deviation between experimental and predicted enhancement factors using the termolecular-kinetics model of this work.

are shown in Fig. 14. The experimental data were collected over a wide range of operating conditions, temperature from 293 to 333 K, total molarity from 3.0 to 9M, loading from ~ 0.007 to 0.49 mol/mol, and contact time from ~ 0.005 to 0.02 s. It is important to mention that these absorption data are a new set of absorption data, which are different for the ones used for developing the kinetics model. A good agreement was obtained between the experimental and predicted enhancement factor. The AAD%, of the measured enhancement factors from the predicted enhancement factor is 15.9%, with a maximum deviation of 33.5%.

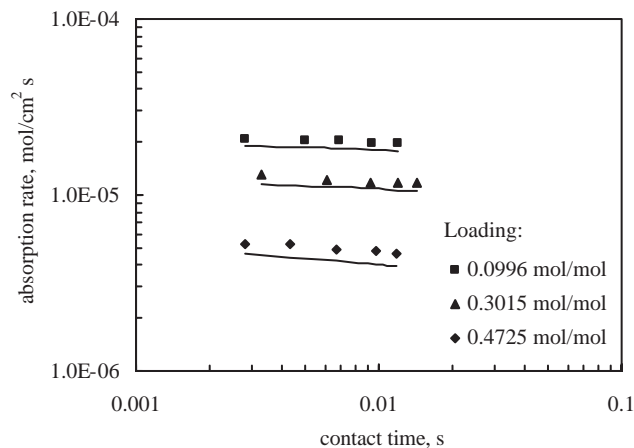


Fig. 15. Measured and predicted absorption rate of CO_2 into aqueous partly loaded 5M MEA solutions at 303 K in laminar jet absorber. Points are measured and lines are predicted by using the termolecular-kinetics model.

As can be seen in Fig. 14, the higher deviations between the measured and predicted data occurred when the concentration of MEA solutions exceed 7 mol/dm^3 of free MEA and when the solution is highly loaded. It should be mentioned that the data obtained at less than 1 mol/dm^3 of free MEA belong to highly loaded solutions. A clearer presentation on the effect of loading on the predictive ability of the model can be shown in Fig. 15. At a loading of about 0.1 and 0.3 mol/mol, the average absolute deviation of the predicted absorption rate from the measured one is 9.3%. This deviation is increased slightly to reach 14.5% as the loading reaches 0.47 mol/mol.

4.2. Kinetics of reaction according to the zwitterion reaction mechanism

The experimental results of the apparent reaction-rate constants (see Fig. 7) show a definite temperature dependence of the overall reaction rate for the five temperatures studied. This is in accord with the literature (Littel et al., 1992) and indicates that the zwitterion formation reaction is most likely to be the rate determining step. The Zwitterion mechanism used to interpret the experimental data of this work is derived from the general form of the zwitterion mechanism (Eq. (13)) by taking the following points into consideration. The contribution to the zwitterion deprotonation by all bases in the solution is possible. Since these deprotonation reactions are fast and instantaneous, their reversibility can be neglected. The k_{app} of the zwitterion mechanism in this case can be presented as in Eq. (45).

$$k_{\text{app}} = \frac{k_4[\text{RNH}_2]}{1 + (k_4/(k_{\text{RNH}_2}[\text{RNH}_2] + k_{\text{H}_2\text{O}}[\text{H}_2\text{O}] + k_{\text{OH}^-}[\text{OH}^-] + k_{\text{HCO}_3^-}[\text{HCO}_3^-] + k_{\text{CO}_3^-}[\text{CO}_3^-]))} \quad (45)$$

The nonlinear regression procedure according to the modified Levenberg–Marquardt algorithm was applied to find the fitting parameters of this equation using the experimental kinetics data at each temperature. The subroutine called DBCLSF documented in the IMSL MATH/library (Visual Numerics Inc., 1994a) was used to obtain the optimum fitting parameters, because this algorithm has been proven to be very efficient in estimating the mass-transfer parameters, as reported elsewhere (Ji et al., 1999). No meaningful values could be estimated for all or any of the six parameters, k_4 , k_{RNH_2} , $k_{\text{H}_2\text{O}}$, k_{OH^-} , $k_{\text{HCO}_3^-}$, $k_{\text{CO}_3^-}$. It has been reported that if the second term in the denominator is comparable to 1, no accurate values for the k_4 parameter can be obtained (Blauwhoff et al., 1984). The ‘Bronsted Relationship’ between the zwitterion-formation rate constant, k_4 , and the acid dissociation constants, pK , of the alkanolamine was found to be valid over a wide range of temperatures for a wide variety of alkanolamines including the primary amine MEA (Versteeg and van Swaaij, 1988). As a result, k_4 can be calculated by Eq. (46), which was developed by Versteeg and van Swaaij (1988) in which its validity over the temperature range of 293–333 K has been confirmed by Littel et al. (1992).

$$\ln k_4 = pK - \frac{7188}{T} + 16.26, \quad (46)$$

where the k_4 in this equation alone is in $\text{m}^3/\text{mol s}$, T is in K, and the pK values can be obtained from the published dissociation constants of Perrin (1965). Again the nonlinear regression analysis conducted on the experimental k_{app} data gave meaningless values for the rest of the five parameters. In addition, the average absolute deviation between the experimental and predicted k_{app} using the obtained parameters was always greater than 60%.

On the other hand, if the second term in the denominator is $\ll 1$, a simple second-order kinetics results, $k_{\text{app}} = k_4[\text{RNH}_2]$ and $r_{\text{CO}_2\text{-MEA}} = k_4[\text{RNH}_2][\text{CO}_2]$. This mechanism was assumed in all the previous literature in the case of $\text{CO}_2\text{-MEA}$ system, as mentioned by Blauwhoff et al. (1984) and Versteeg et al. (1996). This has also proven to be valid only at low concentrations (series-A data), and within the temperature range of 293–313 K, as presented earlier in this paper (see Table 3). Conversely, if the second term is $\gg 1$, the expression in Eq. (47) is the result.

$$k_{\text{app}} = (k_{\text{RNH}_2}[\text{RNH}_2] + k_{\text{H}_2\text{O}}[\text{H}_2\text{O}] + k_{\text{OH}^-}[\text{OH}^-] + k_{\text{HCO}_3^-}[\text{HCO}_3^-] + k_{\text{CO}_3^-}[\text{CO}_3^-])[\text{RNH}_2]. \quad (47)$$

When all the experimental k_{app} constants were fitted to this zwitterion mechanism by a multiple linear regression procedure, only two parameters were found for the optimum fit of the experimental data, k_{RNH_2} and $k_{\text{H}_2\text{O}}$. This means that the deprotonation of the zwitterion were completed only with

the $[\text{RNH}_2]$ and $[\text{H}_2\text{O}]$ species implying that the hydroxyl, carbonate, and bicarbonate ions played no role in the deprotonation of the zwitterion. The results of this analysis are the same as those of the termolecular mechanism (see Table 4). From this, it can be concluded that all the observed phenomena of CO_2 absorption into highly loaded and concentrated MEA solutions can be explained by the termolecular mechanism developed and discussed in Section 4.1.

5. Conclusion

A new termolecular-kinetic model (Eqs. (42)–(44)) has been developed for the CO_2 reaction with MEA solution. Using this kinetics model, the predicted behavior of CO_2 absorption into highly CO_2 loaded and concentrated MEA solution was found to be in accord with the experimental behavior obtained in the laminar jet absorber. In addition, it has been proven that the parameters of this new kinetic model (Eqs. (42) and (43)) can accurately predict published kinetics data at low concentrations and low loadings according to the termolecular reaction mechanism. Furthermore, the termolecular-kinetic model, together with the aid of a numerically solved absorption model has been used to accurately predict, for the first time, CO_2 absorption into high CO_2 loaded and highly concentrated aqueous MEA solutions.

Notation

C_j	concentration of component j in the liquid, mol/dm ³
d	jet diameter, cm
D_j or D	diffusivity of component j , cm ² /s
E	enhancement factor, dimensionless
h	jet length, cm
He	Henry's law constant, kPa dm ³ /mol
k	second order reaction-rate constant, dm ³ /mol s
k_b	second order reaction-rate constant for base B, dm ³ /mol s
k_{app}	apparent pseudo-first-order reaction-rate constant, 1/s
k_i	first or second order reaction-rate constant of reaction i , 1/s or dm ³ /mol s
k_j	first or second order reaction-rate constant of component j , 1/s or dm ³ /mol s
$k_{\text{H}_2\text{O}}$	third order reaction rate constant for H_2O , dm ⁶ /mol ² s
k_{RNH_2}	third order reaction rate constant for MEA, dm ⁶ /mol ² s
K_j or K_i	equilibrium constant of component j or reaction number i
k_L^0	physical mass transfer coefficient, cm/s
L	liquid flow rate, cm ³ /s

N_j	mass transfer flux of j , mol/s cm ² interfacial area
n	reaction order
P_j	partial pressure of j , kPa
r_i or r	reaction rate of reaction i , mol/dm ³ s
T	temperature, K
t	time, s
x	spatial variables measured from the interface into the liquid bulk, cm
$[j]$	concentration of component j , mol/dm ³

Greek letters

α	loading, mol CO_2 /mol MEA
τ	contact time, s

Subscripts

0	initial condition
app	apparent
ave	average condition
e	equilibrium
exp	experimental
i	interface or designated number for reactions
j	generalized component j
pred	predicted

Superscripts

*	property at the gas–liquid interface, interfacial condition
0	bulk condition

Acknowledgements

“The financial supports provided by Natural Sciences and Engineering Research Council of Canada (NSERC), International Test Center for CO_2 Capture (ITC) and Faculty of Engineering, University of Regina are greatly acknowledged. The first author (A. Aboudheir) also appreciates the scholarship support from Canadian Bureau for International Education (Libyan Educational Program).

References

- Aboudheir, A., 2002. Kinetics, modeling, and simulation of carbon dioxide absorption into highly concentrated and loaded monoethanolamine solutions. Ph.D. Thesis, Regina, University of Regina, Canada.
- Aboudheir, A., Tontiwachwuthikul, P., Chakma, A., Idem, R., 2003. On the numerical modeling of gas absorption into reactive liquids in a laminar jet absorber. Canadian Journal of Chemical Engineering, 81 (3/4), 604–612.
- Al-Ghawas, H., Hagewiesche, D., Ruiz-Ibanez, G., Sandall, O., 1989. Physicochemical properties important for carbon dioxide absorption in aqueous methyl-diethanolamine. Journal of Chemical & Engineering Data 34, 385–391.

- Alper, E., 1990. Reaction mechanism and kinetics of aqueous solutions of 2-amino-2-methyl-1-propanol and carbon dioxide. *Industrial and Engineering Chemistry Research* 29, 1725–1728.
- Alvarez-Fuster, C., Midoux, N., Laurent, A., Charpentier, J.C., 1980. Chemical kinetics of the reaction of carbon dioxide with amines in pseudo m - n th order conditions in aqueous and organic solutions. *Chemical Engineering Science* 35, 1717–1723.
- Astarita, G., 1961. Carbon dioxide absorption in aqueous monoethanolamine solutions. *Chemical Engineering Science* 16, 202–207.
- Astarita, G., 1967. *Mass Transfer with Chemical Reaction*. Elsevier Publishing Company, New York.
- Astarita, G., Savage, D., Bisio, A., 1983. *Gas treating with chemical solvents*. Wiley, New York.
- Austgen, D.M., Rochelle, G.T., 1991. Model of vapor–liquid equilibria for aqueous acid gas-alkanolamine systems. Representation of H₂S and CO₂ solubility in aqueous MDEA and CO₂ solubility in aqueous mixtures of MDEA with MEA or DEA. *Industrial and Engineering Chemistry Research* 30, 543–555.
- Austgen, D.M., Rochelle, G.T., Peng, X., Chen, C., 1989. Model of vapor–liquid equilibria for aqueous acid gas-alkanolamine systems using the electrolyte-NRTL equation. *Industrial and Engineering Chemistry Research* 28, 1060–1073.
- Barakat, H.Z., Clark, J.A., 1966. On the solution of the diffusion equation by numerical methods. *Journal of Heat Transfer, Transactions of ASME* 88, 421–427.
- Barth, D., Tondre, C., Delpuech, J., 1986. Stopped-flow investigations of the reaction kinetics of carbon dioxide with some primary and secondary alkanolamines in aqueous solutions. *International Journal of Chemical Kinetics* 18, 445–457.
- Blauwhoff, P.M., Versteeg, G.F., van Swaaij, W.M., 1984. A study on the reaction between CO₂ and alkanolamines in aqueous solutions. *Chemical Engineering Science* 39 (2), 207–225.
- Brian, P.L.T., Vivian, J.E., Matiatos, D.C., 1967. Interfacial turbulence during the absorption of carbon dioxide into monoethanolamine. *A.I.Ch.E. Journal* 13 (1), 28–36.
- Clarke, J.K.A., 1964. Kinetic of absorption of carbon dioxide in monoethanolamine solutions at short contact times. *Industrial and Chemical Engineering Fundamentals* 3 (3), 239–245.
- Crooks, J.E., Donnellan, J.P., 1989. Kinetics and mechanism of the reaction between carbon dioxide and amines in aqueous solution. *Journal of Chemical Society of Perkin Transactions II*, 331–333.
- Danckwerts, P.V., 1970. *Gas Liquid Reactions*. McGraw-Hill, New York.
- Danckwerts, P.V., 1979. The reaction of CO₂ with ethanolamines. *Chemical Engineering Science* 34, 443–446.
- Danckwerts, P.V., Sharma, M.M., 1966. Absorption of carbon dioxide into solutions of alkalis and amines (with some notes on hydrogen sulphide and carbonyl sulphide). I. *Chem. E. Review series, No.2* *Chemical Engineering*, October, CE244–CE280.
- Deshmukh, R.D., Mather, A.E.A., 1981. Mathematical model for equilibrium solubility of hydrogen sulfide and carbon dioxide in aqueous alkanolamine solutions. *Chemical Engineering Science* 36, 355–362.
- Donaldson, T.L., Nguyen, Y.N., 1980. Carbon dioxide reaction kinetics and transport in aqueous amine membranes. *Industrial & Engineering Chemistry Fundamentals* 19, 260–266.
- Edwards, J.T., Maurer, G., Newman, J., Prausnitz, J.M., 1978. Vapor–liquid equilibria in multicomponent aqueous solutions of volatile weak electrolytes. *A.I.Ch.E. Journal* 24 (6), 966–976.
- Emmert, R.E., Pigrord, R.L., 1962. Gas absorption accompanied by chemical reaction: a study of the absorption of carbon dioxide in aqueous solutions of monoethanolamine. *A.I.Ch.E. Journal* 8 (2), 171–175.
- Glasscock, D.A., Critchfield, J.E., Rochelle, G.T., 1991. CO₂ absorption/desorption in mixtures of methyl-diethanolamine with monoethanolamine or diethanolamine. *Chemical Engineering Science* 46 (11), 2829–2845.
- Hagewiesche, D.P., Ashour, S.S., Al-Ghawas, H.A., Sandall, O.C., 1995. Absorption of carbon dioxide into aqueous blends of monoethanolamine and *n*-methyl-diethanolamine. *Chemical Engineering Science* 50 (7), 1071–1079.
- Hikita, H., Asai, S., Ishikawa, H., Honda, M., 1977. The kinetics of reaction of carbon dioxide with monoethanolamine, diethanolamine and triethanolamine by a rapid mixing method. *Chemical Engineering Journal* 13, 7–12.
- Hikita, H., Asai, S., Katsu, Y., Ikuno, S., 1979. Absorption of carbon dioxide into aqueous monoethanolamine solutions. *A.I.Ch.E. Journal* 25 (5), 793–800.
- Horng, S., Li, M., 2002. Kinetics of absorption of carbon dioxide into aqueous solutions of monoethanolamine + triethanolamine. *Industrial and Engineering Chemistry Research* 41, 257–266.
- Ji, X., Kritpiphat, W., Aboudheir, A., Tontiwachwuthikul, P., 1999. Mass transfer parameter estimation using optimization technique: case study in CO₂ absorption with chemical reaction. *Canadian Journal of Chemical Engineering* 77, 69–73.
- Kent, R.L., Eisenberg, B., 1976. Better data for amine treating. *Hydrocarbon Processing*, February 87–90.
- Ko, J., Tsai, T., Lin, C., Wang, H., Li, M., 2001. Diffusivity of nitrous oxide in aqueous alkanolamine solutions. *Journal of Chemical & Engineering Data* 46, 160–165.
- Laddha, S.S., Danckwerts, P.V., 1981. Reaction of CO₂ with ethanolamines: kinetics from gas-absorption. *Chemical Engineering Science* 36, 479–482.
- Leder, F., 1971. The absorption of CO₂ into chemically reactive solutions at high temperature. *Chemical Engineering Science* 26, 1381–1390.
- Li, Y., Mather, A.E., 1994. Correlation and prediction of the solubility of carbon dioxide in a mixed alkanolamine solution. *Industrial and Engineering Chemistry Research* 33, 2006–2025.
- Littel, R.J., Versteeg, G.F., Swaaij, W.M., 1992. Kinetics of CO₂ with primary and secondary amines in aqueous solutions-II. Influence of temperature on zwitterion formation and deprotonation rates. *Chemical Engineering Science* 47 (8), 2037–2045.
- Liu, Y., Zhang, L., Watanasiri, S., 1999. Representing vapor–liquid equilibrium for an aqueous MEA–CO₂ system using the electrolyte nonrandom-two-liquid model. *Industrial and Engineering Chemistry Research* 38, 2080–2090.
- More, J., Garbow, B., Hillstrom, K., 1980. *User Guide for MINPACK-1*. Argonne National Labs Report ANL-80-74, Illinois.
- Penny, D., Ritter, T., 1983. Kinetic study of reaction between carbon dioxide and primary amines. *Journal of Chemical Society Faraday Transactions* 79, 2103–2109.
- Perrin, D.D., 1965. *Dissociation Constants of Organic Bases in Aqueous Solution*. Butterworths, London.
- Pinsent, B., Pearson, J., Roughton, J., 1956. The kinetics of combination of carbon dioxide with hydroxide ions. *Transactions of Faraday Society* 52, 1512–1520.
- Rinker, E.B., Ashour, S.S., Sandall, O.C., 1996. Kinetics and modeling of carbon dioxide absorption into aqueous solutions of diethanolamine. *Industrial and Engineering Chemistry Research* 35, 1107–1114.
- Sada, E., Kumazawa, H., Butt, M.A., 1976a. Gas absorption with consecutive chemical reaction: absorption of carbon dioxide into aqueous amine solutions. *Canadian Journal of Chemical Engineering* 54, 421–424.
- Sada, E., Kumazawa, H., Butt, M.A., Hayashi, D., 1976b. Simultaneous absorption of carbon dioxide and hydrogen sulfide into aqueous monoethanolamine solutions. *Chemical Engineering Science* 31, 839–841.
- Sada, E., Kumazawa, H., Butt, M., Lozano, J., 1977. Interfacial turbulence accompanying chemical reaction. *Canadian Journal of Chemical Engineering* 55, 293–296.
- Sada, E., Kumazawa, H., Han, Z.Q., Matsuyama, H., 1985. Chemical kinetics of the reaction of carbon dioxide with ethanolamine in non-aqueous solvents. *A.I.Ch.E. Journal* 31 (8), 1297–1303.

- Savage, D.W., Kim, C.J., 1985. Chemical kinetics of carbon dioxide reactions with diethanolamine and diisopropanolamine in aqueous solutions. *A.I.Ch.E. Journal* 31 (2), 296–301.
- Sharma, M.M., 1965. Kinetics of reactions of carbonyl sulphide and carbon dioxide with amines and catalysis by bronsted bases of the hydrolysis of COS. *Transactions of Faraday Society* 61, 681–688.
- Shen, K., Li, M., 1992. Solubility of carbon dioxide in aqueous mixtures of monoethanolamine with methyldiethanolamine. *Journal of Chemical & Engineering Data* 37, 96–100.
- Snijder, E.D., te Riele, M.J., Versteeg, G.F., van Swaaij, W.P., 1993. Diffusion coefficients of several aqueous alkanolamine solutions. *Journal of Chemical & Engineering Data* 38, 475–480.
- Song, J., Park, S., Yoon, J., Lee, 1996. Solubility of carbon dioxide in monoethanolamine + ethylene glycol + water and monoethanolamine + poly (ethylene glycol) + water. *Journal of Chemical & Engineering Data* 41 (3), 497–499.
- Tontiwachwuthikul, P., Meisen, A., Lim, C.J., 1992. CO₂ absorption by NaOH, monoethanolamine and 2-amino-2-methyl-1-propanol solutions in a packed column. *Chemical Engineering Science* 47, 381–390.
- Tsai, T., Ko, J., Wang, H., Lin, C., Li, M., 2000. Solubility of nitrous oxide in alkanolamine aqueous solutions. *Journal of Chemical & Engineering Data* 45, 341–347.
- Versteeg, G.F., van Dijk, L.A., van Swaaij, P.M., 1996. On the kinetics between CO₂ and alkanolamines both in aqueous and non-aqueous solutions, An overview. *Chemical Engineering Communications* 144, 113–158.
- Versteeg, G.G., van Swaaij, W.M., 1988. On the kinetics between CO₂ and alkanolamines both in aqueous and non-aqueous solutions-I. Primary and secondary amines. *Chemical Engineering Science* 43 (3), 573–585.
- Visual Numerics Inc., 1994a. IMSL MATH/LIBRARY: FORTRAN Subroutines for Mathematical Applications. Visual Numerics Inc., Texas.
- Visual Numerics Inc., 1994b. IMSL STAT/LIBRARY: FORTRAN Subroutines for Statistical Applications. Visual Numerics Inc., Texas.
- Wang, Y.W., Xu, S., Otto, F.D., Mather, A.E., 1992. Solubility of N₂O in alkanolamines and mixed solvents. *Chemical Engineering Journal* 48, 31–40.
- Weiland, R., Dingman, J., Cronin, D., Browning, G., 1998. Density and viscosity of some partially carbonated aqueous alkanolamine solutions and their blends. *Journal of Chemical & Engineering Data* 43, 378–382.
- Xiao, J., Li, C., Li, M., 2000. Kinetics of absorption of carbon dioxide into aqueous solutions of 2-amino-2-methyl-1-propanol + monoethanolamine. *Chemical Engineering Science* 55, 161–175.